



## OPEN Feasibility and histological analysis of multi-hole versus fully covered self-expandable metallic stents in a porcine model of hilar biliary obstruction

Eui Joo Kim<sup>1,12</sup>, Huapyeong Kang<sup>1,2,12</sup>, Jae Keun Park<sup>3</sup>, Sung Woo Ko<sup>4</sup>, Suk Pyo Shin<sup>5</sup>, Joon Mee Kim<sup>6</sup>, Makoto Kobayashi<sup>7</sup>, Mamoru Takenaka<sup>8</sup>, Sung Ill Jang<sup>9,11</sup>✉ & Seok Jeong<sup>10</sup>✉

Conventional fully covered self-expandable metallic stents (FCSEMS) for hilar biliary obstruction (HBO) remains limited due to the potential for side branch obstruction. The multi-hole covered self-expandable metallic stent (MHSEMS) was designed to overcome the limitations of FCSEMS by incorporating side holes into the fully covered membrane. This preclinical study evaluated the feasibility and safety of MHSEMS compared to conventional FCSEMS in a porcine HBO model. HBO was induced via intraductal radiofrequency ablation in eight minipigs. After four weeks, animals were randomized to receive either an MHSEMS or a conventional FCSEMS and were monitored for 12 weeks. Outcomes included technical success, adverse events, stent removability, and histological analysis. Excluding two procedure-related mortalities (one in each group), technical success and 12-week stent removability were achieved in all animals ( $n = 6$ ). Compared to the FCSEMS group, the MHSEMS group demonstrated trends toward lower total bilirubin levels and reduced histological inflammation score in contralateral ducts (median [range]: 7.5 [7.0–9.0] vs. 9.0 [8.0–10.0], Cliff's delta = 0.67). In conclusion, the MHSEMS was safely and completely removable within a clinically relevant timeframe. This preclinical pilot study suggests a possible signal toward lower histologic injury with the MHSEMS compared with the FCSEMS, supporting the need for larger, adequately powered clinical studies.

A biliary stricture is defined as a narrowing within the biliary system that impedes antegrade bile flow, leading to upstream biliary dilation, inflammation, impaired liver function, and other pathological consequences of obstruction. Biliary obstruction continues to pose a significant clinical challenge and requires effective therapeutic interventions to restore bile flow and prevent complications such as cholangitis and liver abscesses. Historically, surgery was the primary treatment for patients with biliary strictures or obstruction. However, less than 30% of malignant biliary obstructions are surgically resectable at the time of diagnosis<sup>1,2</sup>. Coupled with increasing concerns regarding procedure-related complications and the need to improve patient quality of life, various

<sup>1</sup>Division of Gastroenterology, Department of Internal Medicine, Gachon University Gil Medical Center, Gachon University College of Medicine, Incheon, Korea. <sup>2</sup>Division of Gastroenterology, Department of Internal Medicine, Severance Hospital, Yonsei University College of Medicine, Seoul, Korea. <sup>3</sup>Division of Gastroenterology and Hepatology, Department of Internal Medicine, Hallym University Kangnam Sacred Heart Hospital, College of Medicine, Hallym University, Seoul, Korea. <sup>4</sup>Department of Internal Medicine, Eunpyeong St. Mary's Hospital, College of Medicine, The Catholic University of Korea, Seoul, Korea. <sup>5</sup>Digestive Disease Center, CHA Bundang Medical Center, CHA University School of Medicine, Seongnam, Korea. <sup>6</sup>Department of Pathology, Inha University Hospital, Inha University College of Medicine, Incheon, Korea. <sup>7</sup>Department of Gastroenterology, Yokkaichi Municipal Hospital, Yokkaichi, Japan. <sup>8</sup>Department of Gastroenterology and Hepatology, Kindai University Faculty of Medicine, Osaka, Japan. <sup>9</sup>Department of Internal Medicine, Gangnam Severance Hospital, Yonsei University College of Medicine, Seoul, Korea. <sup>10</sup>Department of Internal Medicine, Inha University Hospital, Inha University College of Medicine, 27 Inhang-ro, Jung-gu, Incheon 22332, Korea. <sup>11</sup>Department of Internal Medicine, Gangnam Severance Hospital, Yonsei University College of Medicine, 211 Eonju-ro, Gangnam-gu, Seoul 06273, Korea. <sup>12</sup>These authors contributed equally: Eui Joo Kim and Huapyeong Kang. ✉email: aerojsi88@gmail.com; inos@inha.ac.kr

minimally invasive techniques have been developed. Percutaneous transhepatic biliary drainage (PTBD), which involves the percutaneous insertion of a catheter proximal to the obstruction, to externally drain bile, offers an effective nonsurgical approach for biliary decompression. Although PTBD offers a high technical success rate, particularly in cases of failed endoscopic retrograde cholangiopancreatography (ERCP) or complex hilar obstruction, it carries significant limitations. These include the need for external catheter placement, which can significantly impair patient quality of life, ongoing external bile loss, increased infection risk, and the potential for peritoneal seeding in malignant biliary obstruction<sup>3</sup>. In contrast, ERCP enables internal biliary drainage—via endoscopic nasobiliary drainage or endoscopic retrograde biliary stent placement—thereby preserving more physiologic bile flow. More recently, endoscopic ultrasound-guided biliary drainage (EUS-BD) has emerged as a novel, minimally invasive alternative. Despite its potential benefits, EUS-BD remains technically demanding, is supported by limited long-term data, and is currently recommended for experienced endoscopists due to the risk of serious complications.

Among the available treatment options, endoscopic stenting has become the primary therapeutic approach due to its minimally invasive nature and proven clinical efficacy<sup>4</sup>. The development of self-expandable metallic stents (SEMS) has significantly advanced the management of both benign and malignant biliary strictures. However, despite numerous comparative studies, no single SEMS type has demonstrated clear superiority. As a result, clinicians must individualize stent selection based on patient-specific factors and the underlying pathophysiology of the stricture<sup>5</sup>.

The anatomical complexity of the perihilar region – marked by the proximity of critical biliary bifurcations and frequent involvement of secondary ducts – presents a unique clinical challenge, and conventional stent designs are often suboptimal. Post-ERCP cholangitis occurs in up to 21.5% of patients following endoscopic stenting for malignant hilar biliary obstruction (HBO)<sup>6</sup>. Although fully covered SEMS (FCSEMS) have demonstrated effectiveness in managing extrahepatic biliary obstructions, their use in perihilar strictures is associated with an increased risk of side branch occlusion, potentially worsening outcomes and contributing to complications such as cholangitis or cholecystitis.

Multi-hole SEMS (MHSEMS), designed with targeted modifications in stent architecture and membrane configuration, including multiple side holes, aims to mitigate side branch obstruction—a major limitation of FCSEMS in the management of perihilar obstruction. This design preserves segmental ductal drainage while maintaining resistance to migration and ensuring adequate stent patency. We hypothesized that MHSEMS would reduce side branch inflammation and facilitate safe removability compared with FCSEMS. However, direct histological evaluation of undrained intrahepatic ducts (IHD) after perihilar stenting is ethically and technically impractical in patients. Obtaining tissue from non-drained side branches would require biopsy or resection of non-tumor-bearing liver parenchyma solely for research purposes. In addition, a substantial proportion of patients with malignant HBO are not candidates for curative resection, and even when surgery is performed, specimens are obtained from tumor-bearing segments rather than from undrained side branches. Accordingly, an animal model is uniquely suited to characterize the histological response of side branches and adjacent hepatic tissue after MHSEMS placement, thereby providing essential preclinical safety data to support future hilar-level clinical evaluation. To investigate this hypothesis, we conducted a preclinical study to evaluate the feasibility and safety of MHSEMS in swine models of HBO.

## Materials and methods

### Animals

Eight female minipigs (*Sus scrofa*; body weight, 25–30 kg) were obtained from Cronex Co., Ltd. (Cheongju, Republic of Korea) for in vivo experiment. All methods were carried out in accordance with relevant guidelines and regulations and this study is reported in accordance with ARRIVE guidelines (<https://arriveguidelines.org>). The study protocol was approved by the Institutional Animal Care and Use Committee (BIOSTEP IACUC 24-HB-0157) prior to initiation. All procedures were conducted at the large animal endoscopy laboratory of HLB BioSTEP Co., Ltd. (Incheon, Republic of Korea). The animals were housed in pathogen-free facilities and maintained in accordance with established guidelines for the use of laboratory animals. Before the commencement of the experiments, all minipigs were subjected to a 7-day quarantine and acclimatization period under standardized environmental conditions (humidity: 55 ± 15%; temperature: 23 ± 3 °C). They were fasted for 24 h before the endoscopic procedure, with unrestricted access to water.

### Endoscopic procedures

All endoscopic procedures were conducted by six biliary endoscopists, each with more than five years of clinical experience in ERCP. Procedures were conducted using a standard therapeutic duodenoscope (TJF-240; Olympus Optical Co. Ltd., Tokyo, Japan). A wire-guided cannulation of the bile duct was performed under fluoroscopic guidance using a 0.035-inch guidewire (Jagwire™; Boston Scientific Corporation, Natick, MA, United States) following endoscopic intubation of the duodenum. Subsequently, a diagnostic cholangiogram was obtained using a cannula (MTW-Endoskopie, Wesel, Germany) to confirm selective bile duct cannulation. All procedures were conducted under general anesthesia. Following sedation with intramuscular xylazine hydrochloride (2 mg/kg), tiletamine-zolazepam (5 mg/kg), and atropine sulfate (0.04 mg/kg), the animals were endotracheally intubated. General anesthesia was maintained throughout the procedure via continuous inhalation of 1.5% isoflurane (Foran; JW Pharmaceutical Corp., Republic of Korea). Procedures were initiated with the animals in the left decubitus position on a fluoroscopy table and transitioned to the prone position after successful selective bile duct cannulation.

### HBO animal model

Perihilar biliary stricture was induced using intraductal radiofrequency ablation (ID-RFA). An ID-RFA catheter (ELRA™ RF catheter; STARmed Co., Ltd., Goyang, Republic of Korea) was introduced over the guidewire into the common hepatic duct (CHD) or proximal common bile duct (CBD) under fluoroscopic guidance. ID-RFA was performed using an RF generator (VIVA combo; STARmed Co., Ltd., Goyang, Republic of Korea) with a setting of 7 W at 80 °C for 120 s. An 11-mm ID-RFA probe catheter was used to apply ablation at the CHD or proximal CBD, with the goal of creating a Bismuth type I or type II perihilar biliary stricture. The intended stricture length was approximately 10 mm.

The left IHD was chosen for the procedure due to its relatively large diameter in minipigs, which allowed for the safe deployment of a 7-Fr ID-RFA catheter. Following successful ID-RFA, a cholangiogram was performed to detect any immediate adverse events, such as contrast leak or pneumoperitoneum suggestive of perforation. Given that perihilar bile duct strictures accompanied by jaundice have been reported following RFA in previous studies, a 7-Fr double-pigtail plastic biliary stent (Zimmon biliary stent; Cook Medical, Bloomington, IN, USA) was placed after each successful ID-RFA procedure to mitigate the risk of unintended mortality in the animal subjects<sup>7</sup>.

During the 4 weeks following ID-RFA and plastic stent placement, the animals were maintained on their routine diet. Four weeks after the ID-RFA procedure, to confirm the presence of HBO, the plastic stent was removed, and deep biliary cannulation followed by cholangiography was performed prior to stent deployment to assess the degree of the ID-RFA-induced stricture (Supplementary Fig. S1). Biliary stricture was defined as a  $\geq 50\%$  reduction in luminal diameter at the site of ID-RFA application compared to baseline, accompanied by dilation of the IHDs proximal to the stricture. Procedure-related adverse events were prospectively recorded.

### Stenting procedure and materials

The MHSEMS (HANAROSTENT™ Multi-Hole™ Biliary; M.I. Tech, Pyeongtaek, Republic of Korea) used in our study is a modified form of FCSEMS. The stent is composed of a nitinol wire mesh and covered with a silicone membrane featuring 1.8-mm perforations in alternating cells along its length (Fig. 1). The first-generation MHSEMS featured 2.5-mm holes in every cell, whereas the second-generation model was designed with 1.8-mm holes in every other cell. This modification aimed to reduce friction with the bile duct wall by decreasing the hole size and to prevent excessive tissue ingrowth or embedding, thereby facilitating stent removal; the stent has a diameter of 6 mm and a rounded margin, with no flares at either end<sup>8</sup>. A 6-mm diameter fully covered self-expandable metal stent (FCSEMS) was selected to reflect anatomical and procedural considerations relevant to perihilar biliary obstruction. In perihilar strictures, the distal extrahepatic bile duct segment below the lesion may remain relatively narrow despite upstream intrahepatic ductal dilatation, and bilateral drainage with FCSEMS commonly necessitates side-by-side deployment in clinical practice. Accordingly, placement of larger-diameter (8–10 mm) FCSEMS may be impractical in this context, particularly in an animal model; therefore, a 6-mm diameter stent was used in the present study. The FCSEMS (M.I. Tech, Pyeongtaek, Republic of Korea)

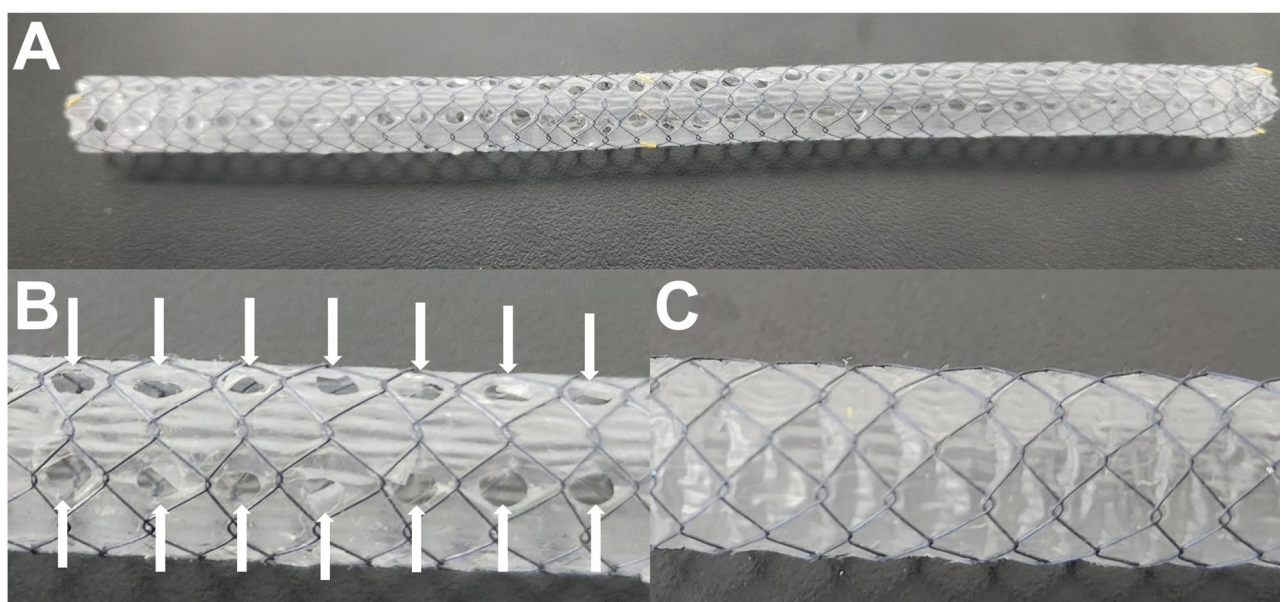


**Fig. 1.** Multi-hole self-expandable metallic stent (MHSEMS). (A) Overview of the MHSEMS in the fully expanded, unconstrained state on the benchtop. (B) Magnified view showing the regularly spaced circular fenestrations created in the polymer covering (white arrows). The fenestrations are aligned in a single longitudinal row and appear approximately every other rhomboid cell of the braided nitinol mesh. (C) Magnified view of a conventional fully covered self-expandable metallic stent.

used in this study is constructed from nitinol wire and fully covered with a silicone membrane. It shares the same design as the MHSEMS but lacks holes in the membrane.

Block randomization with a block size of 8 was performed by a researcher not involved in the procedures to allocate the animal subjects into the MHSEMS and FCSEMS groups. This randomization method was employed to prevent the operator from anticipating the type of stent used in each group or recognizing any allocation patterns between the treatment and control groups. Under fluoroscopic guidance, a single MHSEMS or FCSEMS was deployed across the stricture segment into the left IHD.

### Follow up evaluation and stent removal

Radiologic and laboratory assessments were conducted at baseline (following ID-RFA), 24 h after SEMS exchange (which occurred four weeks after the initial ID-RFA), 4 weeks after SEMS exchange, and at 12 weeks post-SEMS deployment (equivalent to 16 weeks after the initial ID-RFA). These assessments were performed to monitor for adverse events, including acute cholecystitis, stent migration, perforation, and jaundice. At 12 weeks post-SEMS deployment, a follow-up ERCP was performed to assess stent migration and ease of removability. Stent retrieval—either FCSEMS or MHSEMS—was carried out using rat-toothed forceps to grasp and extract the stent through a standard side-viewing endoscope. All procedures were performed by the same endoscopists.

### Outcomes and definitions

Technical success was defined as fluoroscopic confirmation of accurate stent placement across the stricture segment as intended. Because a plastic stent was deployed after stricture formation with ID-RFA, clinical success could not be defined by the resolution of jaundice after SEMS deployment, as in previous studies<sup>8</sup>. Additionally, one prior animal study demonstrated that in species such as dogs, obstruction of up to three-quarters of the liver's bile ducts may not result in clinical jaundice<sup>9</sup>. This suggests that even with partial stent function, jaundice may not manifest during the follow-up period. Based on this information, clinical success in this study was not explicitly defined. However, the number of cases exhibiting aggravated hyperbilirubinemia during the follow-up period after SEMS deployment was recorded. Stent migration was defined as any displacement from the original deployment position across the perihilar stricture, regardless of whether the stent was fully expelled into the bowel or removed from the body.

Upon completion of the experiment, animals were euthanized via intravenous administration of potassium chloride (2 mEq/kg) while under general anesthesia via isoflurane in 100% oxygen administered through an endotracheal tube. Following euthanasia, animals were transferred to the necropsy room for post-mortem examination. The perihilar region, including the liver, gallbladder, and extrahepatic bile ducts, was harvested. The stent-inserted left IHD was marked with a wooden stick to distinguish it from the undrained side-branch IHD. Portions of the perihilar tissue and extrahepatic duct were fixed in 10% neutral buffered formalin. Following deparaffinization and rehydration, paraffin-embedded tissue sections were stained with hematoxylin and eosin (H&E) and Masson's trichrome for histological evaluation. Histological analysis of undrained side branches was performed using a scoring system based on inflammation, neutrophil infiltration, mucosal damage, fibrosis, number of lymphoid follicles, and periductal hepatic parenchymal inflammation (Table 1).

Each histologic parameter was evaluated using predefined criteria to ensure standardized assessment. Inflammation was graded according to its depth and extent: mild inflammation was limited in the mucosal layer, often with pericryptal ("spouse") inflammation; moderate inflammation extended into the muscularis propria; and severe inflammation involved the serosal layer. Neutrophil infiltration was assessed based on presence and severity. A score of 0 indicated the absence of neutrophil infiltration; mild infiltration was characterized by scattered pericryptal neutrophils; moderate by frequent cryptitis; and severe by the presence of multiple crypt abscesses. Mucosal damage was evaluated by estimating the percentage of the affected mucosal thickness relative to the full depth. Damage involving < 30% was classified as mild, 30–60% as moderate, and > 60% as severe. Erosive changes and associated inflammation were recorded separately. Fibrosis was graded semi-quantitatively as mild (score 1), moderate (score 2), or severe (score 3), based on the extent and intensity of collagen deposition. The number of lymphoid follicles was assessed by counting the number of lymphoid follicles per section under medium-power magnification. In addition, the degree of inflammation in the adjacent liver parenchyma was evaluated and classified as mild, moderate, or severe according to the extent of inflammatory cell infiltration. An experienced pathologist who was blinded to the study conditions and groups conducted the analysis.

### Statistical analysis

This experimental pilot study used the minimum number of animals required to test and compare a novel instrument. Data are presented as medians with ranges. Fisher's exact test was used to analyze categorical variables, while the Mann–Whitney U test was employed to compare continuous variables between the two groups. All statistical tests were two-sided, with a significance level set at 0.05. Statistical analyses were performed using SPSS software (version 23.0; IBM Corporation, Armonk, NY, USA) and the statsmodels package in Python.

Score	Inflammation	Neutrophil	Mucosal damage	Fibrosis	Number of lymphoid follicles	Liver parenchymal inflammation
1	Mild	Mild	< 30%	Mild	< 1	Mild
2	Moderate	Moderate	30–60%	Moderate	< 3	Moderate
3	Severe	Severe	> 60%	Severe	< 5	Severe

**Table 1.** Histological scoring system.

Given the small sample size and nonparametric data distribution, effect size was quantified using Cliff's delta<sup>10</sup>. Effect sizes were interpreted as follows: values less than 0.11 indicated a very small or negligible effect; 0.11 to 0.28 indicated a small effect; 0.29 to 0.43 indicated a medium effect; and values greater than 0.43 indicated a large effect. Differences were considered meaningful when the P value was less than 0.05 and accompanied by a medium or large effect size.

## Results

### Development of the HBO animal model

ID-RFA at the CHD or proximal CBD was successfully performed in all eight subjects (Fig. 2). Four weeks after the initial ID-RFA and plastic stent insertion, the plastic stent was successfully removed endoscopically using rat-toothed forceps, and a cholangiogram was performed to confirm the formation of HBO in all eight pigs. After allocation to the treatment groups, either an MHSEMS or an FCSEMS was deployed in the left IHD of each minipig under ERCP guidance.

### Outcomes and removability

In two animals (one in each group), during pre-stent cholangiography performed to confirm HBO formation, the guidewire inadvertently traversed the liver parenchyma proximal to the stricture and entered the peritoneal cavity, with fluoroscopic evidence of contrast extravasation. These two animals were the only cases of mortality during the follow-up period after SEMS placement. At necropsy, both animals exhibited ascites and inflammatory changes within the peritoneal cavity, supporting perforation-related peritonitis as the likely cause of death (Table 2). Excluding these two subjects, no delayed perforations or bleeding were observed in either group. The remaining six minipigs underwent laboratory and radiologic follow-up after SEMS deployment. Baseline laboratory findings were within the normal range in all minipigs. Following SEMS deployment, the

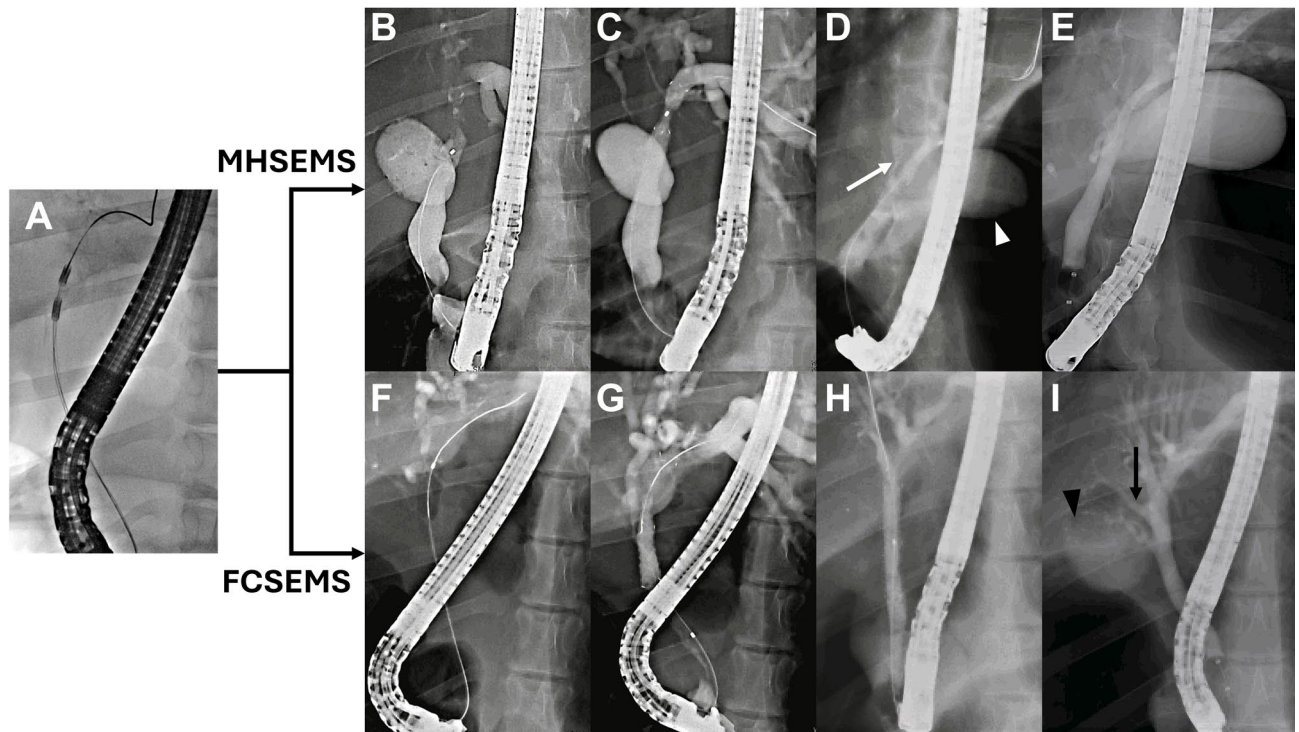


**Fig. 2.** Hilar biliary obstruction (HBO) animal model and cholangiograms during the follow-up period. (A) After successful induction of HBO via intraductal radiofrequency ablation (ID-RFA), either a multi-hole covered self-expandable metallic stent (MHSEMS) or conventional fully covered self-expandable metallic stent (FCSEMS) was deployed according to randomization. (B–E) Case from the multi-hole covered self-expandable metallic stent (MHSEMS) group. (B) Cholangiogram at 4 weeks post-ID-RFA showing perihilar obstruction and left intrahepatic duct (IHD) dilatation. (C) Cholangiogram following MHSEMS deployment across the stricture. (D) Cholangiogram at 12 weeks post-MHSEMS deployment, showing visible, non-dilated right IHD (white arrow) and gallbladder (white arrowhead). (E) Cholangiogram after MHSEMS removal, showing non-dilated right IHD and gallbladder. (F–I) Case from the conventional fully covered self-expandable metallic stents (FCSEMS) group. (F) Cholangiogram showing perihilar obstruction and left IHD dilatation prior to FCSEMS deployment. (G) Cholangiogram following FCSEMS deployment. (H) Cholangiogram at 12 weeks post-FCSEMS deployment showing absence of visible right IHD and gallbladder. (I) Cholangiogram after FCSEMS removal, showing dilated right IHD (black arrow) and gallbladder with cystic duct (black arrowhead).

	MHSEMS (n = 4)	FCSEMS (n = 4)	P
Expire during follow-up, n	1/4	1/4	> 0.999
Perforation by guidewire	1/4	1/4	> 0.999
Bleeding, n	0/4	0/4	NA
Distal stent migration, n	1/3	3/3	0.400
Laboratory findings, post SEMS deployment at 1mo, median (range)			
WBC, x10 <sup>3</sup> /mL	23.44 (18.19–74.42)	14.73 (11.51–43.41)	0.400
Total bilirubin, mg/dL	0.27 (0.27–0.29)	3.62 (0.24–3.86)	0.700
AST, U/L	46.9 (26.8–53.3)	51.4 (20.3–90.7)	> 0.999
ALT, U/L	10.8 (3.5–14.4)	11.3 (7.2–13.9)	> 0.999
ALP, U/L	258.9 (167.7–506.8)	306.0 (235.1–457.2)	> 0.999
Post stenting hyperbilirubinemia, n	0/3	2/3	0.400
Histologic findings, median (range)			
Histologic score	7.5 (7.0–9.0)	9.0 (8.0–10.0)	0.200

**Table 2.** Clinical and histological outcomes.

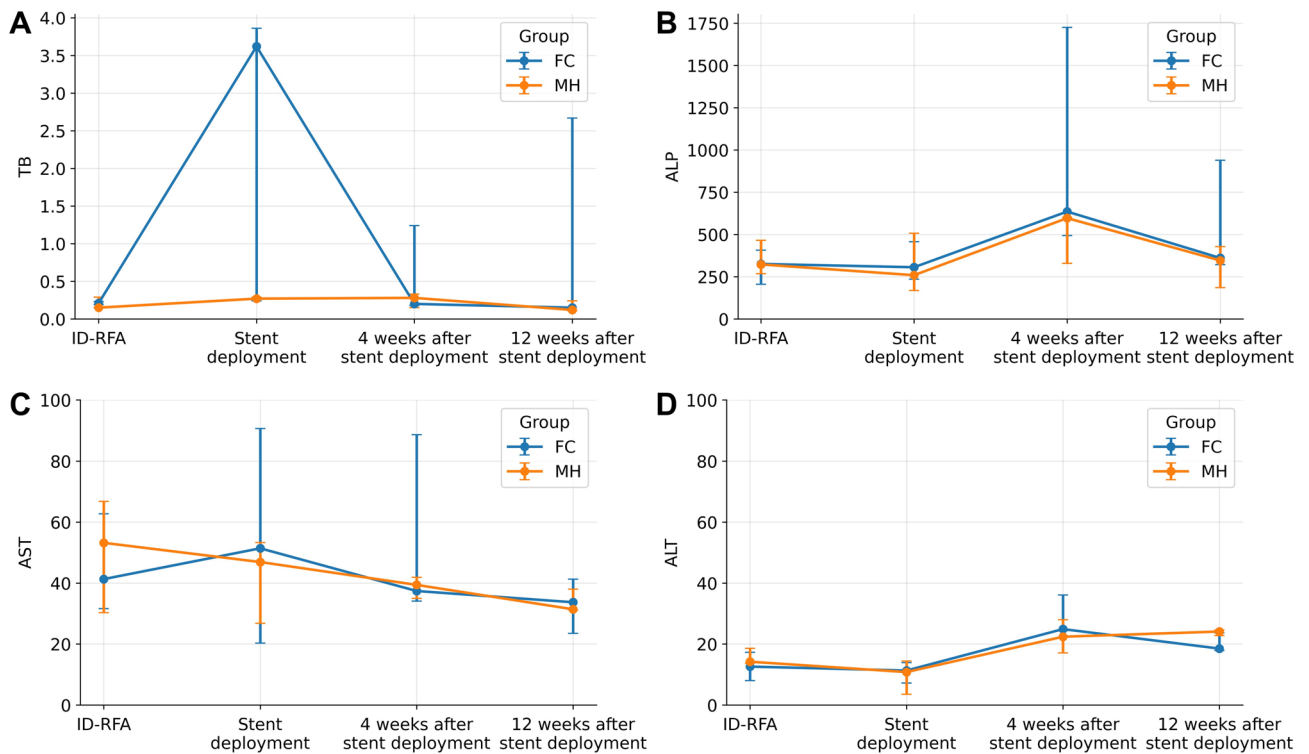


**Fig. 3.** Median values with ranges (error bars) of laboratory parameters during the follow-up period by group. (A) Serum total bilirubin (TB) levels during the follow-up period, with hyperbilirubinemia at 24 h post-self-expandable metallic stent deployment in the conventional fully covered self-expandable metallic stent (FCSEMS) group shown in blue. (B) Serum alkaline phosphatase (ALP), displaying a wide range of values in the FCSEMS group. (C) Serum aspartate aminotransferase (AST) levels, with broad variability across both groups. (D) Serum alanine aminotransferase (ALT) levels, exhibiting a similar temporal pattern in both groups.

MHSEMS group exhibited a trend toward lower total bilirubin levels compared with the FCSEMS group (median [range]: 0.27 [0.27–0.29] vs. 3.62 [0.24–3.86], Cliff’s delta=0.33,  $P=0.700$ ), although statistical significance was not reached. During the follow-up period, hyperbilirubinemia was observed in two of the three subjects in the FCSEMS group, while no cases occurred in the MHSEMS group (Table 2). In the affected animals, hyperbilirubinemia gradually improved over the 12-week period (Fig. 3A). Follow-up ERCP was performed on all six minipigs at 12 weeks after SEMS deployment. SEMS remained within the bile duct in all subjects, although dislocation of the SEMS was observed in one subject from the MHSEMS group and three from the FCSEMS

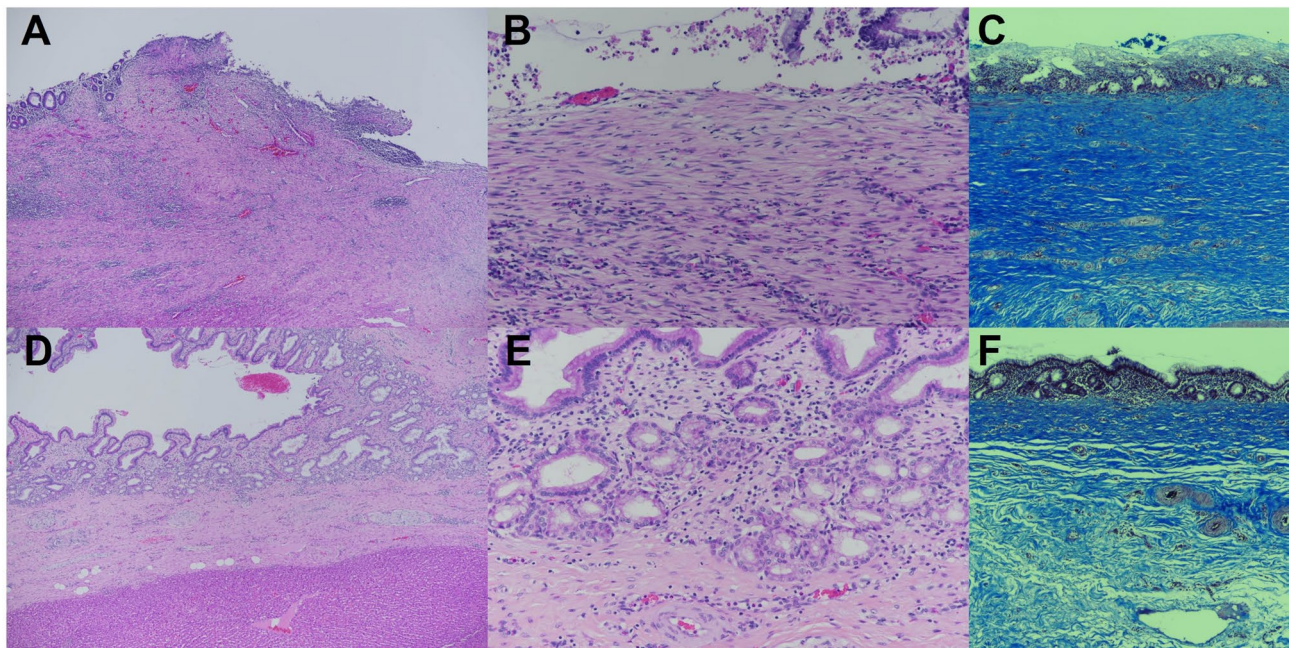


**Fig. 4.** Histological findings of undrained side branches of intrahepatic bile ducts. (A–C) Representative findings from the conventional fully covered self-expandable metallic stents (FCSEMS) group; (D–F) Representative findings from the multi-hole covered self-expandable metallic stent (MHSEMS) group. (A) Dense inflammatory cell infiltration with scattered neutrophils in the mucosa and submucosa, accompanied by epithelial erosions (hematoxylin and eosin [H&E],  $\times 40$ ). (B) Abundant fibrous tissue with scattered inflammatory cells and a denuded epithelial layer (H&E,  $\times 200$ ). (C) Homogenization of the collagen fiber with a broad band of fibrous tissue extending into the underlying hepatic parenchyma (Masson's trichrome,  $\times 100$ ). (D) Well-preserved ductal epithelium with minimal reactive alterations (H&E,  $\times 40$ ). (E) Mildly scattered mononuclear cell infiltration in the biliary mucosa (H&E,  $\times 200$ ). (F) Periductal fibrosis with a thin, reticular pattern (Masson's trichrome,  $\times 100$ ).

group (Table 2). All MHSEMS and FCSEMS were successfully removed endoscopically from all six animals (Supplementary Fig. S2).

### Histological outcomes

Following successful SEMS removal in both groups, the six minipigs were euthanized for histological evaluation (Fig. 4). Perihilar specimens were successfully obtained from all subjects, and histological slides were prepared from undrained branch ducts adjacent to the SEMS deployment area for evaluation using the predefined histological scoring system (Table 1). Although not statistically significant, MHSEMS showed a consistent reduction in inflammation score with a large effect size (median [range]: 7.5 [7.0–9.0] vs. 9.0 [8.0–10.0], Cliff's delta = 0.67,  $P = 0.200$ ), suggesting a potential reduction in the risk of side branch occlusion and associated inflammation; however, this difference did not reach statistical significance (Table 2).

### Discussion

This preclinical comparative animal study evaluated the safety and efficacy of MHSEMS for HBO, specifically assessing improvements in segmental cholangitis, stent patency, and removability. As a preclinical pilot trial, the findings did not reveal statistically significant differences between groups, but the histological examination scores revealed histologic trend suggesting functional drainage preservation with substantial effect sizes, as indicated by Cliff's delta, suggesting potential differences between the MHSEMS and conventional FCSEMS. The lack of statistical significance may be attributed to insufficient statistical power due to the limited sample size rather than a true absence of effect. Some previous clinical studies have demonstrated the effectiveness of MHSEMS in cases of extrahepatic bile duct obstruction, but to date none have investigated histological changes in HBO<sup>11–15</sup>. Therefore, the present study provides novel evidence that has not been addressed in prior research.

Recent advances in endoscopic stenting, a minimally invasive approach, have made it possible to treat a wide range of biliary obstructive diseases that were previously managed through surgical or percutaneous interventions. Among the various types of biliary stents, plastic stents are the most widely used due to their clinical effectiveness, ease of placement, and cost-efficiency. Most plastic stents are designed with side holes to allow drainage of side branches and feature anchoring flaps to reduce the risk of stent migration. However, a significant disadvantage of plastic stents is their relatively short stent patency duration, often due to the formation of bacterial biofilms or the accumulation of biliary sludge, which can lead to recurrent cholangitis or jaundice<sup>16,17</sup>.

SEMS have been developed with a larger luminal diameter compared to plastic stents to prolong stent patency<sup>18,19</sup>. The structure of SEMS consists of long tubular mesh made from metal alloys such as stainless steel, Elgiloy, and nitinol<sup>20</sup>. The use of metal alloys in the mesh provides adequate radial force, enhancing the effectiveness of biliary stricture treatment. Although SEMS are generally more expensive than plastic stents, their superior stent patency duration makes them more cost-effective in the long term<sup>21,22</sup>. A retrospective study found that while fenestrated plastic stents had comparable survival and adverse event rates, they had inferior patency compared to uncovered SEMS (UCSEMS)<sup>23</sup>. Additionally, SEMS outperformed plastic stents in terms of reintervention rates, symptom palliation, and patient survival in cases of HBO<sup>24,25</sup>.

However, SEMS also have several disadvantages. UCSEMS have reduced migration rates compared to FCSEMS, but they are more prone to tissue ingrowth, which can lead to recurrent stent occlusion. In patients with HBO, UCSEMS can be bilaterally deployed into both IHDs using the Y-shaped stent-in-stent technique or the side-by-side technique. However, recent advancements in systemic chemotherapy and immunotherapy have led to prolonged survival in patients with malignant HBO, making reintervention following initial biliary drainage with UCSEMS a significant clinical challenge.

In contrast, FCSEMS mitigate this risk through complete mucosal coverage, preventing tissue ingrowth. Moreover, since FCSEMS do not become embedded, they can be readily removed or replaced. However, they introduce new challenges, such as higher migration rates and the potential for side branch obstruction. This latter complication is particularly concerning in anatomical configurations where the cystic duct or IHD originates near the stricture site, as this may lead to cholecystitis or cholangitis<sup>26</sup>. Partially covered SEMS were developed to combine the benefits of both designs, but clinical evidence has failed to demonstrate consistent improvements in stent patency or complication profiles<sup>27–29</sup>.

According to the literature, acute cholecystitis associated with stent placement has been documented in up to 12% of patients treated with FCSEMS for biliary stricture treatment, highlighting a significant complication associated with FCSEMS<sup>30</sup>. Notably, in patients with malignant biliary strictures, FCSEMS are associated with a higher risk of acute cholecystitis compared to UCSEMS (7.8% vs. 1.2%;  $P < 0.001$ )<sup>31</sup>. This complication is an important consideration in the management of patients with biliary strictures, particularly those at risk of side branch blockage.

The perihilar region presents significant anatomical challenges for FCSEMS placement due to the presence of IHD side branches. The use of FCSEMS in this area is highly restricted, requiring either prior cholecystectomy, bilateral side-by-side placement extending to both main IHDs, or acceptance of potential side branch obstruction, which can lead to complications such as cholangitis or liver abscess. A retrospective study involving FCSEMS for HBO reported a liver abscess incidence rate of 7%<sup>32</sup>. Furthermore, when deploying more than two stents, the diameter of the stents may be reduced, potentially compromising stent patency. Based on this evidence, the most recent guidelines for malignant HBO recommend the use of plastic stents in patients expected to undergo long-term systemic therapy, such as chemotherapy, noting that SEMS should be reserved for patients with a limited life expectancy ( $< 3$  months), where minimizing the need for reintervention is a priority<sup>5,33</sup>.

This therapeutic challenge prompted the development of MHSEMS, designed to overcome the limitations of FCSEMS while retaining their advantages. Early clinical trials focusing on distal bile duct obstructions demonstrated that MHSEMS significantly reduced migration rates compared with conventional FCSEMS, suggesting potential improvements in stent patency<sup>33</sup>. However, data on patency duration remain inconsistent across studies, with some reports indicating comparable or even shorter patency periods relative to FCSEMS<sup>12</sup>.

Notably, MHSEMS incorporate design modifications to minimize side branch occlusion; these may provide particular advantages in perihilar strictures, where the risk of cystic duct or IHD obstruction is higher with FCSEMS compared to distal bile ducts. However, clinical evidence supporting the use of MHSEMS for managing HBO remains limited. One animal study involving the first-generation MHSEMS reported a 100% success rate in stent placement without any adverse events; the stent's design also enabled safe removal within 1 month, addressing a common limitation associated with UCSEMS<sup>34</sup>. In the present study, we validated the feasibility and safety of the second-generation MHSEMS for HBO over a 3-month duration.

Animal studies are a crucial preclinical phase for assessing safety and efficacy before human trials, but they cannot definitively replicate malignant obstructions in patients. The animal model used in this study more closely resembles benign strictures rather than malignant pathology. However, the lack of validated preclinical animal models that accurately mimic malignant biliary strictures limits the ability to conduct more advanced preclinical investigations beyond those performed in this study. Given that the benign biliary stricture model may produce results that differ from the clinical presentation of malignant biliary tract obstructions, further clinical research will be essential to validate the efficacy of MHSEMS in malignant HBO, building on the foundation established by this preclinical study.

The outcomes from our long-term preclinical animal study indicate that endoscopic biliary drainage of HBO using the MHSEMS is technically feasible and safe. The MHSEMS may offer a therapeutic option for managing HBO, effectively preventing side branch obstruction while maintaining adequate stent patency. Although bilateral stenting is typically favored to achieve drainage of  $> 50\%$  of liver volume, unilateral stenting may be necessary in certain clinical scenarios. In such cases, MHSEMS has the potential to provide substantial clinical advantages by achieving effective drainage of  $> 50\%$  of the liver volume using a single stent. This approach is particularly advantageous in patients with Klatskin tumors classified as Bismuth type I or II, where a single MHSEMS is anticipated to achieve sufficient drainage<sup>5</sup>. However, in clinical practice, Klatskin tumors of type III and IV—which are more commonly encountered among perihilar obstructions—raise concerns regarding the adequacy of biliary decompression with a single MHSEMS. Further studies are warranted to evaluate its clinical efficacy across these subtypes. In particular, clinical validation in patients with various subtypes of malignant HBO is required to determine whether unilateral or bilateral drainage with this MHSEMS is superior.

The primary limitation of this study is the small sample size ( $n = 6$ ; 3 animals per group), which substantially limits statistical power. Accordingly, the between-group comparisons for lab findings and histological scores did not reach statistical significance, and any apparent between-group differences should be interpreted with caution. Although we reported effect sizes using Cliff's delta to describe the magnitude and direction of observed differences, effect size estimates in small cohorts remain imprecise and do not establish superiority. Therefore, the present findings should be considered preliminary and hypothesis-generating. Second, procedure-related mortality occurred in two animals during pre-stent cholangiography performed to confirm HBO formation, in which the guidewire inadvertently traversed the liver parenchyma and entered the peritoneal cavity with fluoroscopic contrast extravasation. Because these events occurred before stent deployment and one case occurred in each group, they are most consistent with model- and technique-related complications rather than a device-specific safety signal; nevertheless, such instability may confound feasibility and safety assessments in small cohorts. Finally, our ID-RFA-induced HBO animal model does not replicate malignant tumor biology. Consequently, this model cannot evaluate tumor ingrowth through the stent fenestrations/side holes, which is a clinically important mechanism of recurrent obstruction in malignant hilar biliary disease.

In conclusion, in this porcine model of HBO, MHSEMS placement and removal were technically feasible within a clinically relevant timeframe. While we observed numerical differences in histological outcomes, the study was underpowered and no statistically significant superiority could be demonstrated. These results should be viewed as preliminary and hypothesis-generating, providing a rationale for further evaluation in larger, adequately powered clinical studies.

### Data availability

The data presented in this study are available on request from the corresponding author.

Received: 6 December 2025; Accepted: 10 February 2026

Published online: 18 February 2026

### References

- Salgado, S. M., Gaidhane, M. & Kahaleh, M. Endoscopic palliation of malignant biliary strictures. *World J. Gastrointest. Oncol.* **8**, 240–247. <https://doi.org/10.4251/wjgo.v8.i3.240> (2016).
- Dorrell, R., Pawa, S. & Pawa, R. Endoscopic management of malignant biliary stricture. *Diagnostics (Basel)* **10** <https://doi.org/10.3390/diagnostics10060390> (2020).
- Molina, H., Chan, M. M., Lewandowski, R. J., Gabr, A. & Riaz, A. Complications of percutaneous biliary procedures. *Semin Intervent Radiol.* **38**, 364–372. <https://doi.org/10.1055/s-0041-1731375> (2021).
- Elmunzer, B. J. et al. ACG clinical guideline: diagnosis and management of biliary strictures. *Am. J. Gastroenterol.* **118**, 405–426. <https://doi.org/10.14309/ajg.0000000000002190> (2023).
- Angsuwatcharakon, P. et al. The updated Asia-Pacific consensus statement on the role of endoscopic management in malignant hilar biliary obstruction. *Endosc Int. Open.* **12**, E1065–E1074. <https://doi.org/10.1055/a-2366-7302> (2024).
- Xia, M. X. et al. The risk of acute cholangitis after endoscopic stenting for malignant hilar strictures: A large comprehensive study. *J. Gastroenterol. Hepatol.* **35**, 1150–1157. <https://doi.org/10.1111/jgh.14954> (2020).
- Cho, J. H. et al. Long-term results of temperature-controlled endobiliary radiofrequency ablation in a normal swine model. *Gastrointest. Endosc.* **87**, 1147–1150. <https://doi.org/10.1016/j.gie.2017.09.013> (2018).
- Lee, J. et al. Endoscopic stenting of a fully covered Self-Expandable metal stent with a hole in each cavity in malignant hilar biliary obstruction: A preclinical Proof-of-Concept study and initial human experience. *Dig. Dis. Sci.* **70**, 1215–1222. <https://doi.org/10.1007/s10620-024-08810-1> (2025).
- McMaster, P. D. & Rous, P. The biliary obstruction required to produce jaundice. *J. Exp. Med.* **33**, 731–750. <https://doi.org/10.1084/jem.33.6.731> (1921).
- Berntsen, D. Direct retrieval as a theory of involuntary autobiographical memories: evaluation and future directions. *Memory* **32**, 709–722. <https://doi.org/10.1080/09658211.2023.2294690> (2024).
- Kitagawa, K., Tomooka, F. & Yoshiji, H. Efficacy of a novel covered metallic stent with side holes for malignant anastomotic stenosis of choledochojejunostomy. *Dig. Endosc.* **36**, 628–630. <https://doi.org/10.1111/den.14779> (2024).
- Takeda, T. et al. Outcomes of multi-hole self-expandable metal stents versus fully covered self-expandable metal stents for malignant distal biliary obstruction in unresectable pancreatic cancer. *DEN Open.* **5**, e70014. <https://doi.org/10.1002/deo2.70014> (2025).
- Tanoue, K. et al. Antegrade stenting using a new covered multi-hole metal stent for malignant biliary obstruction in surgically altered anatomy. *Endoscopy* **56**, E98–E99. <https://doi.org/10.1055/a-2233-2843> (2024).
- Maruyama, H. et al. Stent-in-stent deployment above the papilla to treat malignant hepatic hilar biliary obstruction using novel fully covered multi-hole metal stent. *Endoscopy* **55**, E1062–E1064. <https://doi.org/10.1055/a-2158-7776> (2023).
- Ogura, T., Uba, Y., Kanadani, T., Besho, K. & Nishikawa, H. Multi-hole metal stent can prevent cystic and pancreatic duct obstruction during endoscopic ultrasound-guided antegrade stenting combined with hepaticogastrostomy. *Endoscopy* **57**, E163–E164. <https://doi.org/10.1055/a-2528-0340> (2025).
- Vaishnavi, C., Samanta, J. & Kochhar, R. Characterization of biofilms in biliary stents and potential factors involved in occlusion. *World J. Gastroenterol.* **24**, 112–123. <https://doi.org/10.3748/wjg.v24.i1.112> (2018).
- Lee, T. H. Technical tips and issues of biliary stenting, focusing on malignant hilar obstruction. *Clin. Endosc.* **46**, 260–266. <https://doi.org/10.5946/ce.2013.46.3.260> (2013).
- Huibregtse, K., Cheng, J., Coene, P. P., Fockens, P. & Tytgat, G. N. Endoscopic placement of expandable metal stents for biliary strictures—a preliminary report on experience with 33 patients. *Endoscopy* **21**, 280–282. <https://doi.org/10.1055/s-2007-1012969> (1989).
- Irving, J. D. et al. Gianturco expandable metallic biliary stents: results of a European clinical trial. *Radiology* **172**, 321–326. <https://doi.org/10.1148/radiology.172.2.2664861> (1989).
- Chun, H. J. et al. Gastrointestinal and biliary stents. *J. Gastroenterol. Hepatol.* **25**, 234–243. <https://doi.org/10.1111/j.1440-1746.2009.06152.x> (2010).
- Davids, P. H., Groen, A. K., Rauws, E. A., Tytgat, G. N. & Huibregtse, K. Randomised trial of self-expanding metal stents versus polyethylene stents for distal malignant biliary obstruction. *Lancet* **340**, 1488–1492. [https://doi.org/10.1016/0140-6736\(92\)92752-2](https://doi.org/10.1016/0140-6736(92)92752-2) (1992).
- Kaassis, M. et al. Plastic or metal stents for malignant stricture of the common bile duct? Results of a randomized prospective study. *Gastrointest. Endosc.* **57**, 178–182. <https://doi.org/10.1067/mge.2003.66> (2003).

23. Kerdsirichairat, T. et al. Endoscopic drainage of > 50% of liver in malignant hilar biliary obstruction using metallic or fenestrated plastic stents. *Clin. Transl Gastroenterol.* **8**, e115. <https://doi.org/10.1038/ctg.2017.42> (2017).
24. Sangchan, A., Kongkasame, W., Pugkhem, A., Jenwitheesuk, K. & Mairiang, P. Efficacy of metal and plastic stents in unresectable complex hilar cholangiocarcinoma: a randomized controlled trial. *Gastrointest. Endosc.* **76**, 93–99. <https://doi.org/10.1016/j.gie.2012.02.048> (2012).
25. Mukai, T. et al. Metallic stents are more efficacious than plastic stents in unresectable malignant hilar biliary strictures: a randomized controlled trial. *J. Hepatobiliary Pancreat. Sci.* **20**, 214–222. <https://doi.org/10.1007/s00534-012-0508-8> (2013).
26. Lee, T. H., Moon, J. H. & Park, S. H. Biliary stenting for hilar malignant biliary obstruction. *Dig. Endosc.* **32**, 275–286. <https://doi.org/10.1111/den.13549> (2020).
27. Lam, R. & Muniraj, T. Fully covered metal biliary stents: A review of the literature. *World J. Gastroenterol.* **27**, 6357–6373. <https://doi.org/10.3748/wjg.v27.i38.6357> (2021).
28. Saito, K. et al. A prospective multicenter study of partially covered metal stents in patients receiving neoadjuvant chemotherapy for resectable and borderline resectable pancreatic cancer: BTS-NAC study. *Gut Liver.* **15**, 135–141. <https://doi.org/10.5009/gnl19302> (2021).
29. Niiya, F. et al. Efficacy and safety of uncovered self-expandable metal stents for distal malignant biliary obstruction in unresectable non-pancreatic cancer. *DEN Open.* **5**, e383. <https://doi.org/10.1002/deo2.383> (2025).
30. Wong, M., Sanchez-Luna, S. A. & Rustagi, T. Endoscopic transpapillary gallbladder stenting to prevent acute cholecystitis in patients receiving FCEMS for benign biliary stricture. *Endosc Int. Open.* **9**, E1386–E1390. <https://doi.org/10.1055/a-1500-8028> (2021).
31. Jang, S. et al. Association of covered metallic stents with cholecystitis and stent migration in malignant biliary stricture. *Gastrointest. Endosc.* **87**, 1061–1070. <https://doi.org/10.1016/j.gie.2017.08.024> (2018).
32. Inoue, T. et al. Feasibility of the placement of a novel 6-mm diameter threaded fully covered self-expandable metal stent for malignant hilar biliary obstructions (with videos). *Gastrointest. Endosc.* **84**, 352–357. <https://doi.org/10.1016/j.gie.2016.03.1501> (2016).
33. Kulpatcharapong, S. et al. Efficacy of multi-hole self-expandable metal stent compared to fully covered and uncovered self-expandable metal stents in patients with unresectable malignant distal biliary obstruction: a propensity analysis. *Surg. Endosc.* **38**, 212–221. <https://doi.org/10.1007/s00464-023-10541-9> (2024).
34. Park, J. S., Jeong, S., Kobayashi, M. & Lee, D. H. Safety, efficacy, and removability of a fully covered multi-hole metal stent in a swine model of hilar biliary stricture: a feasibility study. *Endosc Int. Open.* **7**, E498–E503. <https://doi.org/10.1055/a-0846-0775> (2019).

## Author contributions

Conceptualization, S.I.J., S.J., M.K., M.T.; Study design: S.I.J., S.J.; Methodology: S.I.J., S.J.; Data collections: E. J.K., H.K., J.K.P., S.W.K., S.P.S.; Data analysis: E.J.K., J.M.K.; Writing—original draft: E.J.K.; Writing—review and editing: H.K., J.M.K.; Supervision: S.I.J., S.J.; Project administration: S.J. E.J.K. and H.K. equally contributed to this article as first authors. S.I.J. and S.J. equally contributed to this article as corresponding authors. All authors have read and approved the final version of the manuscript.

## Funding

This research was funded by the 2024 domestic medical device new product association linked user (Medical Institution) multi-institution evaluation support project.

## Declarations

## Competing interests

The authors declare no competing interests.

## Additional information

**Supplementary Information** The online version contains supplementary material available at <https://doi.org/10.1038/s41598-026-40067-8>.

**Correspondence** and requests for materials should be addressed to S.I.J. or S.J.

**Reprints and permissions information** is available at [www.nature.com/reprints](http://www.nature.com/reprints).

**Publisher's note** Springer Nature remains neutral with regard to jurisdictional claims in published maps and institutional affiliations.

**Open Access** This article is licensed under a Creative Commons Attribution-NonCommercial-NoDerivatives 4.0 International License, which permits any non-commercial use, sharing, distribution and reproduction in any medium or format, as long as you give appropriate credit to the original author(s) and the source, provide a link to the Creative Commons licence, and indicate if you modified the licensed material. You do not have permission under this licence to share adapted material derived from this article or parts of it. The images or other third party material in this article are included in the article's Creative Commons licence, unless indicated otherwise in a credit line to the material. If material is not included in the article's Creative Commons licence and your intended use is not permitted by statutory regulation or exceeds the permitted use, you will need to obtain permission directly from the copyright holder. To view a copy of this licence, visit <http://creativecommons.org/licenses/by-nc-nd/4.0/>.

© The Author(s) 2026